First-principles calculations to investigate electronic structure and optical spectra of CdxZn1-xS ternary semiconductor alloys

Article · February 2023

DOI: 10.1016/j.chphi.2023.100177

3 authors:

Benlechheb Soumia
Université de M'sila
1 PUBLICATION **0** CITATIONS
SEE PROFILE

Mustapha Boucenna
Université de M'sila
23 PUBLICATIONS **276** CITATIONS
SEE PROFILE

Nadir Bouarissa
Université de M'sila
385 PUBLICATIONS **5,496** CITATIONS
SEE PROFILE

Chemical Physics Impact xxx (xxxx) 100177

Contents lists available at ScienceDirect

Chemical Physics Impact

journal homepage: www.elsevier.com

Journal Cover Image

First-principles calculations to investigate electronic structure and optical spectra of CdxZn1-xS ternary semiconductor alloys

S. Benlechheb [a], M. Boucenna [a], N. Bouarissa [b, *]

[a] Physics Department, Faculty of Science, University of M'sila, 28000 M'sila, Algeria
[b] Laboratory of Materials Physics and Its Applications, University of M'sila, 28000 M'sila, Algeria

ARTICLE INFO

Keywords:
Structural properties
Electronic structure
Optical spectra
$Cd_xZn_{1-x}S$
Ab initio calculations

ABSTRACT

The structural parameters, electronic band structure and optical spectra of $Cd_xZn_{1-x}S$ ($0 \le x \le 1$) ternary semiconductor alloys are studied. The calculations are realized using the full potential linearized augmented plane wave method. The modified local density approximation (LDA) and generalized gradient approximation (GGA) have been used for describing the exchange-correlation potential. The obtained results for zinc-blende $Cd_xZn_{1-x}S$ ternary alloys show a general wellness with the data shown in the literature. An inspection of electronic band structure indicates that zinc-blende $Cd_xZn_{1-x}S$ are ($\Gamma \rightarrow \Gamma$) direct band gap semiconductors (from $x = 0$ up to $x = 1$). A predominant ionic type of the chemical bonding in these materials has been indicated. The density of states shows various peaks in both valence and conduction localities proposing that an abundance of conditions is obtainable for occupation. The alloys affect the optical features of interest. The results obtained from the present work show that the zinc-blende $Cd_xZn_{1-x}S$ is a promettant material for photovoltaic device applications. Moreover, the alloy of interest can be used in different devices from visible to ultraviolet light.

1. Introduction

II-VI wide-band gap materials with their ternary alloys posed physical properties that are situated between those of semiconductors and insulators. The semiconductors can be applied in different domains for blue and ultraviolet applications [1–9]. Their crystallization is taken to be either in the wurtzite or in the zinc-blende crystal structure [10]. ZnS is an inorganic material. It is the essential form of the zinc present in nature, where it essentially happens as the mineral sphalerite. It belongs to a wide-energy gap II-VI binary semiconductor materials. This material can be doped by both p and n types. It is also very useful in image display applications. The most stable bulk form of ZnS is zinc-blende structure under ambient conditions [11]. ZnS can be transparent, and may be used for visible and infrared optics as a window. It is phosphorescent and this can make it important for several electrical and decorative applications. It can also be used as a pigment for paints, plastics and rubber. On the other hand, similarly to ZnS, the cadmium sulfide (CdS) has two crystal forms. Hexagonal wurtzite structure that represents more stability and cubic zinc-blende one. For both structures, the Cd and S atoms are four coordinates [12]. It is a yellow solid and an another important inorganic material that has many applications in technology. It is reported that chemical precipitation methods give the cubic zinc-blende structure [13]. This is a direct energy gap material [14]. A colored appearance has been given to the nearness of its energy gap to visible light wavelengths [15]. We can also combine CdS within different layers in thin-film form for using it in certain types of solar cells [16].

Larger band-gap and elevated optical transmittance are two essential properties a material must have to proceed as a window layer in a solar cell. CdS is the further extensively worn window material now-a-days. However, CdS absorbs the blue serving of the sunlight and reduces the short-circuit current of the solar cell. By alloying ZnS with CdS, one obtains the ternary alloy cadmium zinc sulfides ($Cd_xZn_{1-x}S$) which have properties in between those of ZnS and CdS. $Cd_xZn_{1-x}S$ is an undertaking candidate for substituting CdS as a window layer [17]. Its optical energy band-gap is comparatively larger than CdS and can be adjusted from 2.42 to 3.60 eV by the checked summation of Zn [18]. Likewise it supplies elevated optical transmittance than CdS that in turning augments the short-circuit current of the solar cell [19–21]. The summation of Zn to the upward of extensively worn CdS buffer layer material improves the electronic and optical properties of optoelectronics apparatuses [22–24]. The $Cd_xZn_{1-x}S$ thin films band structure has a greater energy band gap than CdS. This performs the material much more interesting for manufacturing of solar cells. It has been an exten-

* Corresponding author:
E-mail address: nadir.bouarissa@univ-msila.dz (N. Bouarissa).

https://doi.org/10.1016/j.chphi.2023.100177
2667-0224/

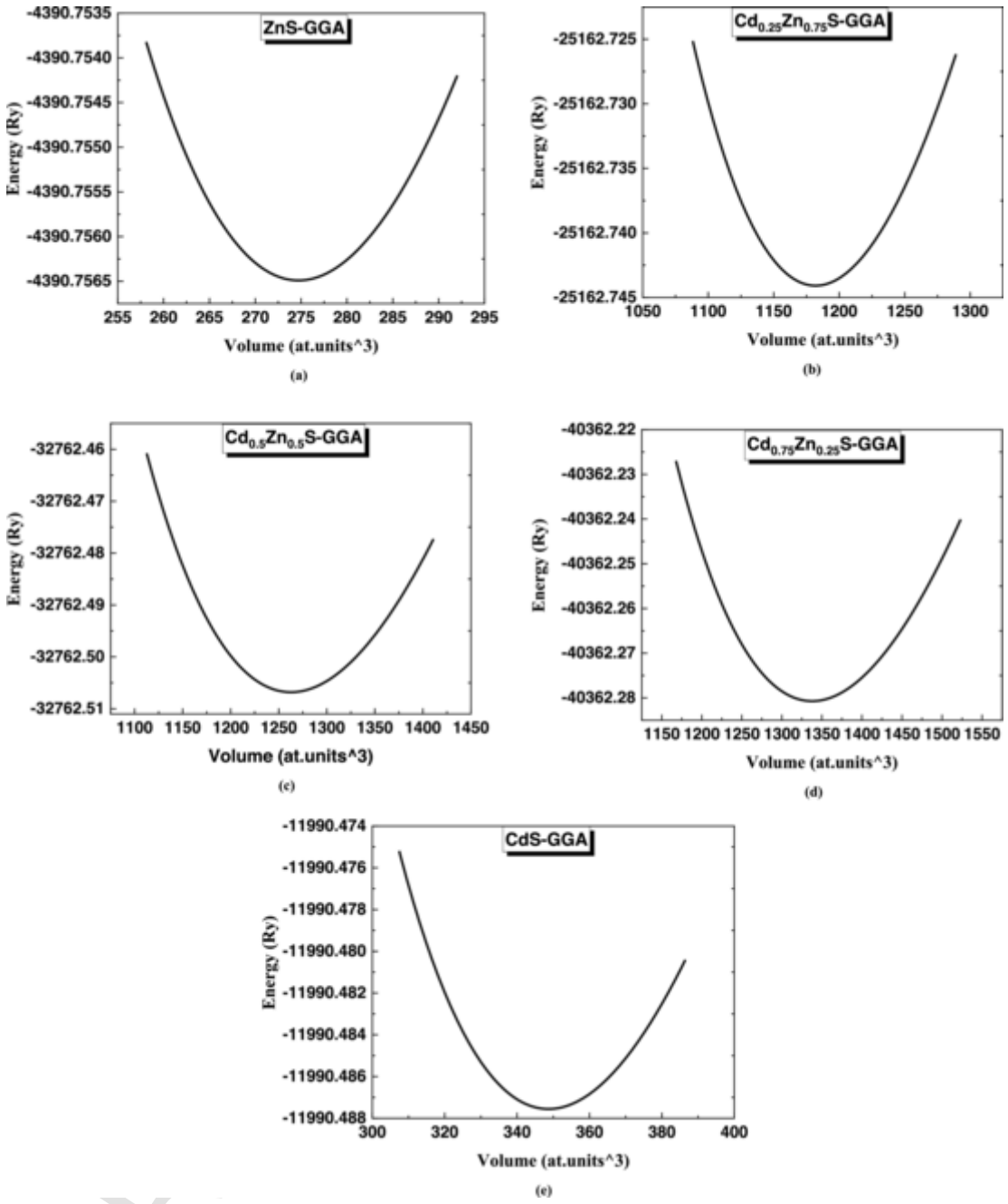

Fig. 1. Total energy versus volume for (a) ZnS (b) $Cd_{0.25}Zn_{0.75}S$ (c) $Cd_{0.50}Zn_{0.50}S$ (d) $Cd_{0.75}Zn_{0.25}S$ and (e) CdS materials obtained from GGA.

sively worn as a broad band gap window material in hetero-junction photovoltaic solar cells and photoconductive devices [22–24]. This material founds several utilizations in hetero-junction solar cells [25–27], in photoconductive devices [28] and in the industries of p-n junction solar cells as window layers [29]. Also, pumped $ZnS/Zn_xCd_{1-x}S$ quantum well lasers are shown to be done [30–32].

The electron structure, optical characteristics, mechanical and thermodynamics properties are very interesting tools for the study of the electronic states and their band parameters [33–36]. A precise understanding of these quantities is required for the design of their waveguides for optimizing their device performances [33–39]. In fact, these properties are interesting for the understanding of the photon-electron interactions. Also, they are very interesting for the determination of the microelectronic and optoelectronic of materials for devices [40–51]. The accurate knowledge of these properties plays a crucial function for the evaluation of these materials quality and in the design and manufacture of optoelectronic implements formed on them.

In spite of the importance of these properties for $Cd_xZn_{1-x}S$ semiconductor ternary alloys, only a few is known about them, according to the information we have [52–55]. This has advised us to investigate the constitutional parameters, energy bands and optical spectrum of the alloy of interest in the zinc-blende structure for x varying from 0 to 1. The focus of the present study is to give supplementary information to the facts available in the biography. The objective of the present work is to demonstrate how these characteristics of concern vary when changing the parameter x from 0 up to 1, i.e. to express the performance of all investigated quantities as a function of the alloy composition x. Actually, the variation of x in $Cd_xZn_{1-x}S$ semiconductor ternary alloys pushes to the change in the physical, chemical and structural characteristics that this material undergoes when varying the composition x. This may hap-

Table 1
Calculated equilibrium lattice constant (in Å) for zinc-blende $Cd_xZn_{1-x}S$ ternary semiconductor alloys using LDA, LDA-spin and GGA approximations compared with experiment and other theoretical calculations .

Zinc-blende				
Approximation	**X**	**$a_{Present}$ (Å)**	**$a_{Theo.}$ (Å)**	**$a_{Exp.}$ (Å)**
	0	5.4607	5.30 [67]	5.420 [66]
GGA	0.25	5.594	–	–
	0.50	5.719	–	–
	0.75	5.82	–	–
	1	5.910	5.80 [68]	5.8320 [66]
LDA	0	5.3188	–	5.420 [66]
	0.25	5.4459	–	–
	0.50	5.5631	–	
	0.75	5.6536	–	–
	1	5.7507	–	5.8320 [66]
LDA-spin	0	5.32	–	5.420 [66]
	0.25	5.446	–	–
	0.50	5.56	–	–
	0.75	5.666	–	–
	1	5.745	–	5.8320 [66]

pen when we examine the features of interest with priority on their confidence on the concentration x of the alloy under study and opens new proprieties which permits to have novel fundamental properties of materials. The work has been conducted from ab initio full-potential linearized augmented plane wave (FP-LAPW) method within both a linear density approximation (LDA) and a generalized gradient approximation (GGA). This method with different exchange potentials has also been used by Kaur et al. [56] in order to find the structural stability of Rh_2XZn (X = Mn, Zn) full-Heusler compounds as well as their transport and thermodynamic properties. Thus, the motivation of the present work is to find new electronic properties and optical spectra that have not been reported for neither ZnS nor CdS. In the next section of the present paper, we give more specification about the methodology used in the calculations.

2. Computational details

The attending ab initio calculations are substantially coming from the density functional theory (DFT) [57,58] using the FP-LAPW method as accomplished within the WIEN2k code [59]. The exchange-correlation potential is used through LDA and GGA approximations. In the present case, each unit cell has been split into an interstitial region and non-overlapping muffin-tin spheres (MTS) of radii R_{MT} . In the MTS, the wave functions are expanded using a linear combination of radial atomic functions time spherical harmonics, whereas in the Infrared, a plane wave basis set has been used. Using the method of conjugate gradient, the energy function of Kohn-Sham has been minimized directly. The R_{MT} that is pointed out the shortest muffin-tin sphere radius is shipment to be 1.9 atomic units for Zn and Cd atoms and 1.8 atomic units for S atom. A grid of $10\times10\times10$ meshes are utilized for sampling the Brillouin zone formed on the scheme by Monkhorst and Pack [60,61]. A cutoff plane wave of $R_{MT}.k_{max}=7$ has been appropriated. k_{max} shows the greatness of the maximum k vector in the plane wave expansion. We have also been calculated the electronic structure by solving first the equation of Kohn-Sham, and minimizing after the total energy with respect to moderation of electrons, ions, and unit cell parameters in a accordant process. These calculated parameters have been taken to ensure that the error of the total energy is 0.1 mRy. In the present working, the periodic supercells has also been used where the out coming alloy is a random mixture of Zn and Cd in the zinc-blende anion sites whereas S in the zinc-blende cation sites. The global lattice constant of the alloy is engaged with undertaking Vegard's law [62],

$$a_{CdZnS} = x a_{CdS} + (1-x)\, a_{ZnS} \quad (1)$$

where a_{CdS} and a_{ZnS} are the lattice constants of the zinc-blende CdS and ZnS materials, respectively.

The optical properties of a material can be upsurge by the complex dielectric function $\varepsilon(\omega) = \varepsilon_1(\omega) + i\varepsilon_2(\omega)$, that is immediately linked to the linear reply of matter to incident radiation. The imaginary part $\varepsilon_2(\omega)$ of the complex dielectric function, that characterizes the absorption of the incident light by the matter, can be estimated by summing all permitted direct electronic transitions from occupied to unoccupied states [63]. The real part of $\varepsilon_1(\omega)$the dielectric function, that perfects the dispersion of the incident radiations by the matter, can be derived from the imaginary part $\varepsilon_2(\omega)$ via the Kramer–Kronig transformation [64].

3. Results and discussion

3.1. Structural properties

The understanding of the lattice parameter is needed in materials science investigation. Normally, this parameter is acquired by determining the total energy per primitive unit cell versus the volume for the materials under consideration [65]. The obtained energy-volume details have been fitted using the Murnaghan's equation of state. The equilibrium volume dependence of the total energy of the zinc-blende for ZnS, $Cd_{0.25}Zn_{0.75}S$, $Cd_{0.50}Zn_{0.50}S$, $Cd_{0.75}Zn_{0.25}S$ and CdS have been obtained. Here, we present only our results using GGA method as shown in Fig. 1. However, in Table 1 we present also the data obtained by using the LDA and LDA-spin methods as well. The outcomes concerning the equilibrium lattice constant a_0 for various calculated structures at zero pressure taking Cd contents of 0%, 25%, 50%, 75% and 100% are illustrated in table 1. The existing experiments and theoretical data are also communicated for comparison. The table shows that our calculations using the GGA approach overestimate the experimental equilibrium lattice parameter [66] by lower than 1% for ZnS ($x = 0$) and 2% for CdS ($x = 1$). They are also overestimated with respect to the theoretical ones reported in Refs. [67,68]. Our obtained lattice parameters using LDA and LDA spin approaches is underestimated with respect to experiment. Note that the experimental results are acquired at room temperature and our merits neglect the thermal expansion. We think that the best method to be chosen here is the GGA approach.

3.2. Electronic properties

The energy bands of zinc-blende structures for $Cd_xZn_{1-x}S$ materials for $x = 0$, 0.25, 0.50, 0.75 and 1 are shown in Fig. 2. The calculations have been realized along the high-symmetry directions in the Brillouin zone obtained from the GGA-modified Becke-Johnson (mBJ) [69] exchange potential in the foundation of FP-LAWP as accomplished in the Wien2k collection [59]. The energy reference is taken at zero and corresponds to the Fermi energy. We observe that the general characteristics of energy bands of the major importance are simulate conceptually to each other. A predominant ionic type of the chemical bonding in these materials has been indicated. The Fermi level seems to do not cross the energy bands. This has been checked for all materials being studied here. Therefore, all materials being studied here are semiconductors. For these materials, the maximum of the valence band is revealed at the Γ point in the Brillouin zone and the lowest of the conduction band is located as well at the Γ point in the Brillouin zone. We can then conclude that for all $x = 0$, 0.25, 0.50, 0.75 and 1 materials, all the structures are zinc-blende with Γ structure. These materials differ essentially by their energy band-gaps. Our results concerning the band-gaps for the material under study for the structures of zinc-blende are shown in table 2. Note that the data concerning the zinc-blende structures are balanced with those of Refs. [70,71] and found to be in reasonable agreement for $x = 0$ and $x = 1$ at zero temperature when using the GGA-mBJ method. We note also that there is a big difference between the states at

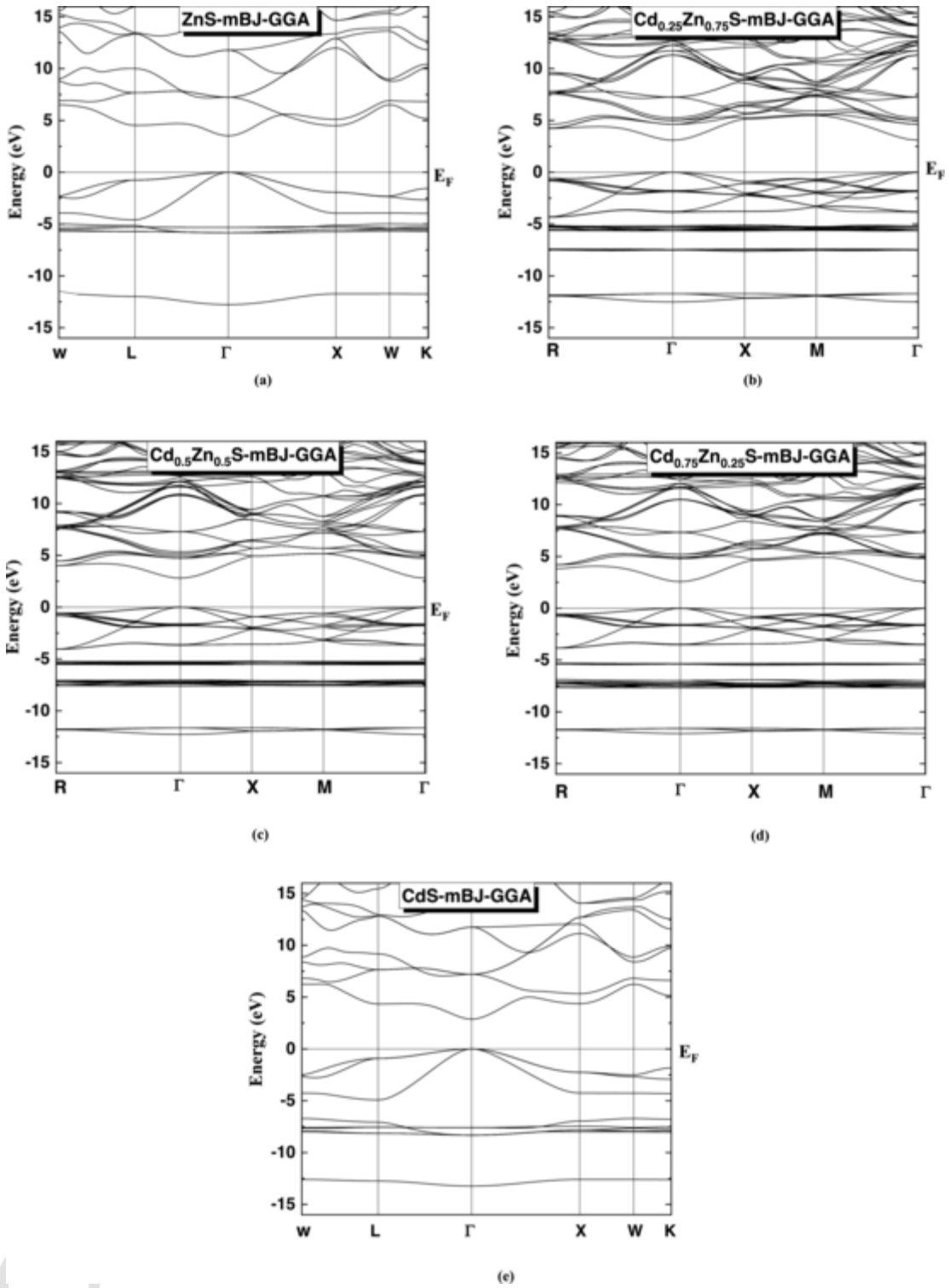

Fig. 2. Electronic band structure for (a) ZnS (b) $Cd_{0.25}Zn_{0.75}S$ (c) $Cd_{0.50}Zn_{0.50}S$ (d) $Cd_{0.75}Zn_{0.25}S$ and (e) CdS materials obtained using mBJ-GGA approximations.

the lowest conduction band and those at the highest valence band. This leads to a slight carrier effective masses and to the enhancement of the electron mobility.

To inspect the beginning of the states in the electronic structure for the investigated materials, the density of states (DOS) have been calculated and their results are discussed. In Fig. 3, we present the DOS of zinc-blende $Cd_xZn_{1-x}S$ semiconducting alloys for $x = 0, 0.25, 0.50, 0.75$ and 1. The results have been presented for both total and partial DOS. The bottom valence band is appeared to be in the majority S atoms with slight contribution of Zn and Cd atoms. The last valence states requires mainly S, with minor donations that comes from Zn and Cd states. A strong hybridization between Zn and Cd and these states in the neighborhood of the Fermi level is essentially in charge of the electronic and superconducting effects of these materials. A further consideration of this figure specifies that the s states commanding the bottom valence band region. The shortest valence band for the zinc-blende structure situated between −0.30 and −0.10 eV posed mostly spx + py and pz2 characters. The piece located between −0.30 to 0 eV is predominantly

Table 2
Energy band-gaps of $Cd_xZn_{1-x}S$ (in eV) as obtained from different approximations in this work.

Composition x	Energy-gaps (eV)			
	GGA	LDA	LDA-spin	mBJ-GGA
0	1.96	2.155	1.717	2.267 3.66 [70]
0.25	1.563	1.5921	1.596	1.98
0.50	1.296	1.4679	1.4706	1.807
0.75	1.113	1.8687	1.358	1.698
1	1.417	1.150	1.052	1.864 2.36 [71]

acquired from S-s electrons. The DOS shows diverse peaks in both valence and conduction regions advocating that an important number of states is accessible for occupation. The GGA-mBJ method has enhanced the intensity of the Zn-3d state and pushed it towards the Fermi level when we compare it with the LDA.

3.3. Optical properties

The optical characteristics of semiconducting materials are predominant substantial portion for expressing the nature of the semiconductor. A valuable information of these properties is required for the depiction of the waveguide to optimize the production of the devices [72–76]. The dielectric function is one of the essential relevant optical characteristics of materials. The real part represents the ability of the material to store the electric energy, or in terms of the ability to permit the electric field through it. It is an interaction of the degree of polarization. The greater is the degree of polarization, the bigger is the value of the real part. On the other hand, the imaginary part represents the loss of energy in the material. It actually indicates the Ohm resistance of the material. It is associated with dielectric losses. The dielectric loss factor is a measure of the energy absorbed in the medium as an electromagnetic wave passes through that medium. Actually, when a semiconductor is submitted to an outside electric field, its degree of polarization is described by the real part of its dielectric function. Also, the imaginary part of the dielectric function demonstrates the quantity of consumption inside the semiconductor under investigation. It comes up with both intra-band and inter-band transitions. In Figs. 4a and 4 b we illustrate the real part (ϵ_1) and the imaginary part (ϵ_2) of the dielectric function for zinc-blende $Cd_xZn_{1-x}S$ ternary alloys, respectively. The x changes in the interval 0–1. We took the values of the concentrations of x as 0, 0.25, 0.50, 0.75 and 1. We observe that the dielectric function ϵ_1 values for the materials of interest are considerable within near and middle ultraviolet sectors but become smaller in the far ultraviolet region (Fig. 4a). We can also see that ϵ_2 begins to augment from the photon energy of about 1 eV until about 6 eV where it becomes plafond (Fig. 4b). This maximum value is obtained for $x = 0$ (i.e. for ZnS). Then, it decreases rapidly until reaching about 14 eV. The same behavior has been shown for distinctive x varying from o up to 1 within small deviations from each other. At around 6 eV (Fig. 4a), there is an essential peak for the real part of zinc-blende $Cd_xZn_{1-x}S$. When the Cd becomes larger, this peak is dislocated on the way to different energies. The location and widen of the censorious peaks have been appeared to be almost constant throughout the Cd concentrations. The introduction of Cd within the variation of the critical points positions leads to a progression between the valence and the elevated conduction bands at both the zone center and along the [111] direction. The position of the peak is decreased and it is moved with regard to the lowest photon energies. It gets more precise when the Cd is increased. This is ascribed to inter-band transitions. The general shape of ϵ_1 is that anticipated for a harmonic oscillator for zinc-blende ZnS and CdS materials. As far as the Cd content in $Cd_xZn_{1-x}S$ is increased, the frequency of resonance is carried with regard to elevated energies. When one goes from pure ZnS to pure CdS, the starting energy of the absorption for ϵ_2 decreases. These points are Γ_v-Γ_c splittings. The great significance of the real part $\epsilon_1(\omega)$ spreads neighboring the ultraviolet energy spectrums shows that these materials under study can be reliably requested in optoelectronic fields.

The reflectivity is an optical criterion that can be attained from the knowledge of the complex dielectric function (ϵ). This parameter has been calculated for $Cd_xZn_{1-x}S$ semiconductor ternary alloys using the GGA process in the photon energy spectrum 1–14 eV. The results have been shown in Fig. 5. We note that a sequences of smaller peaks is seen in the spectrum of the reflectivity of $Cd_xZn_{1-x}S$ alloys when moving from ZnS ($x = 0$) to CdS ($x = 1$). The peaks have been derived from inter-band transitions. The width has been ascribed to the phonon-phonon scattering that has the responsibility for the vibration dampening. The largest of the reflectivity is all over the place 70% along y axis. It is depending on the photon energy range.

The electron energy loss function is also an important optical criterion to be investigated. Usually this parameter is used for describing the energy loss of fast electrons which transverse in a studied material [72]. In Fig. 6 we show the spectra of the energy loss of fast electrons that make a cross in the matter of interest for a given value for x. For zinc-blende $Cd_xZn_{1-x}S$ ternary alloys we use the GGA-approach in the photon energy scope of 1 to 14 eV. In the electronic energy loss function spectra, the peaks report the features which are connected with the plasmon resonance. For the top highlight, the frequencies which coincide with these plasma are explained as plasmon frequency. According to the reports, more than the plasma frequency indicates that the material of interest is a dielectric and lower than it, the material acts like a metallic material apparently [72]. The principal peak of the curve that describes the electron energy loss of $Cd_xZn_{1-x}S$ ternary semiconductor alloys is found at a photon energy of roughly 13 eV for an $x = 1$, i.e. for CdS compound.

For designing and fabricating devices, the refractive index (n) is a useful optical parameter [77–82]. In the current investigation, n(E), E is the energy of the photon, which is obtained for zinc-blende $Cd_xZn_{1-x}S$ ternary alloys using the GGA-approach in the photon energy interval of 1 to 14 eV. The outcome concerning n versus the photon energy are drawn in Fig. 7. An appreciable peaks that are arise from the excitonic transitions at the E_0 borders are noticed. The powerful peak in n(E) spectra which appears at approximately a photon energy of around 6 eV can be connected basically to the 2D exciton transition (E_1). The variation of the Cd atoms affects its position. Thus, the 2D exciton transition (E_1) will be affected. It is to be noted also that the greatest amount of n(E) appears to be at around a photon energy of 5 to 6 eV. It is interrelated with the consummation. We observe that n has a significant importance at low photon energies. However, it decreases quickly at greater photon energies. An appearance of peaks which are arise from the excitonic transitions can be seen. The excitonic outcomes be predisposed to increase the power of the oscillator at M_0 and M_1 points [9,83]. The most important peak in the refractive index diapason is principally associated to the 2D exciton transitions (E_1).

The optical absorption coefficient $\alpha(\omega)$ is one of the compelling estimation indicator of materials for checking their usefulness for utilizing them in the production and manufacturing of photovoltaic implements. In the present contribution $\alpha(\omega)$ has been calculated for zinc-blende $Cd_xZn_{1-x}S$ ternary alloys using the GGA-technique in the photon energy interval 1–14 eV. Fig. 8 displays the change of α versus the photon energy for $Cd_xZn_{1-x}S$ ternary materials. The photon energy is taken to be 0, 0.25, 0.50, 0.75 and 1 as shown in Fig. 8. We observe that the highest value of $\alpha(\omega)$ for $Cd_xZn_{1-x}S$ ternary alloys takes place for a photon energy of approximately 9 eV. The concerned materials have absorption bands from about 1.50 to about 14 eV. It accommodates considerable peaks. The great absorption takes place between about 6 and 14 eV and is dependent on the absorbed light energy. A big optical absorption coefficient ($> 10^4$ cm^{-1}) has been noticed. This has been done with a broad absorption band for the compound of interest. For the fact that

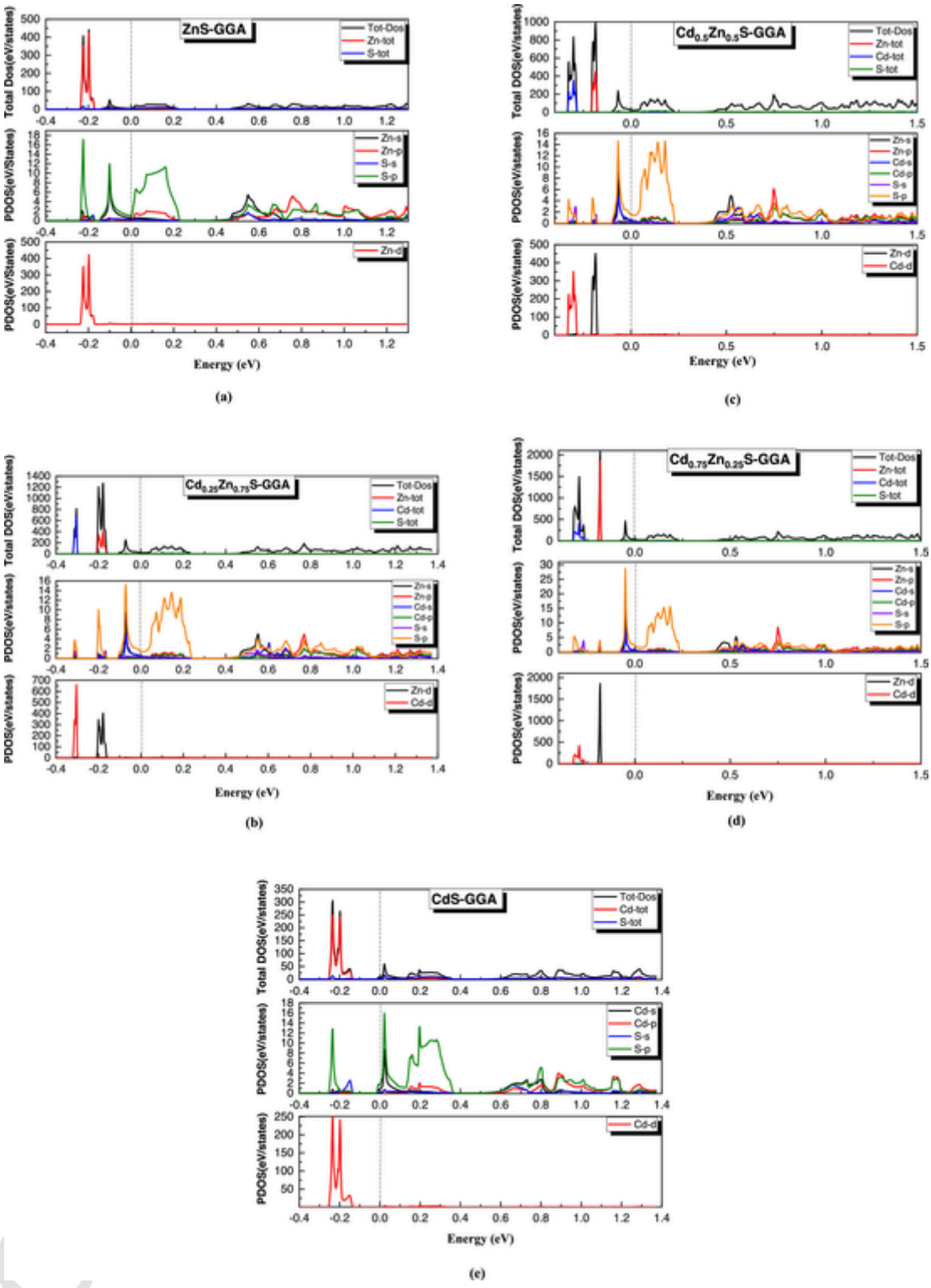

Fig. 3. Partial and total density of states for (a) ZnS (b) $Cd_{0.25}Zn_{0.75}S$ (c) $Cd_{0.50}Zn_{0.50}S$ (d) $Cd_{0.75}Zn_{0.25}S$ and (e) CdS materials obtained using mBJ-GGA approximations.

the solar radiation be a member of the visible and infrared light sectors and the big absorption grows the solar cell productivity, we can look forward to that $Cd_xZn_{1-x}S$ ternary alloys are good candidate materials for photovoltaic applications.

4. Conclusions

In summary, the structural properties, electronic band structure, and optical spectra of zinc-blende $Cd_xZn_{1-x}S$ ternary semiconductor alloys were investigated using the FP-LAPW method. The exchange-correlation potential was reported by using the GGA within the mBJ improvement. Results regarding lattice constant parameters for $Cd_xZn_{1-x}S$

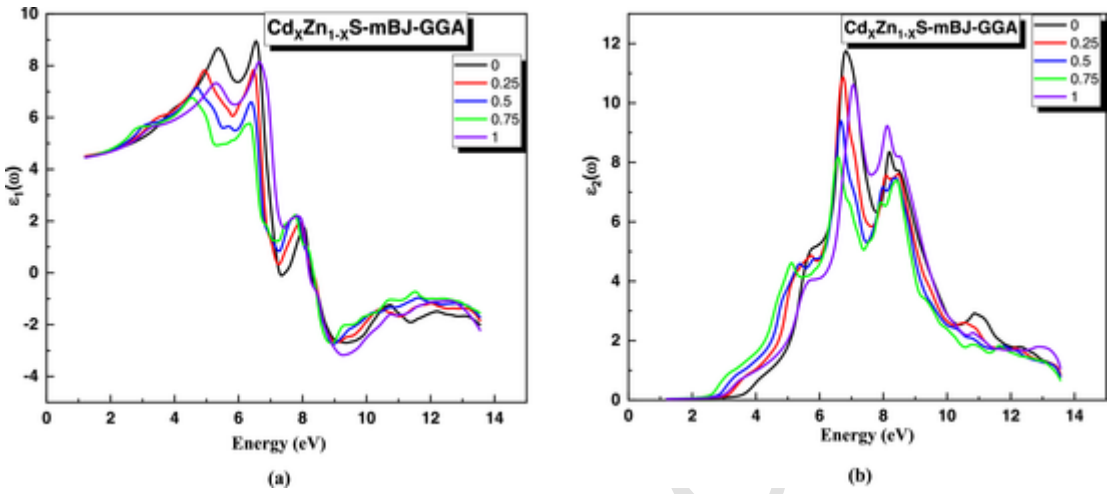

Fig. 4. (a) Real and (b) imaginary parts of the dielectric function for $Cd_xZn_{1-x}S$ using mBJ-GGA method for $x = 0$, 0.25, 0.50, 0.75 and 1.

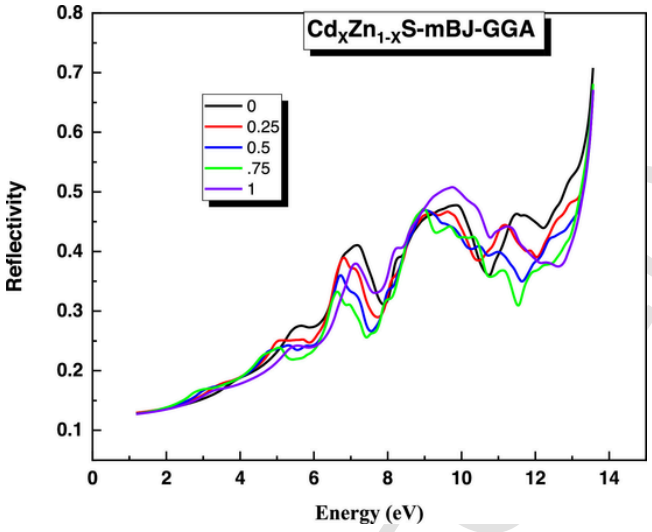

Fig. 5. Reflectivity for $Cd_xZn_{1-x}S$ using mBJ-GGA method for $x = 0$, 0.25, 0.50, 0.75 and 1.

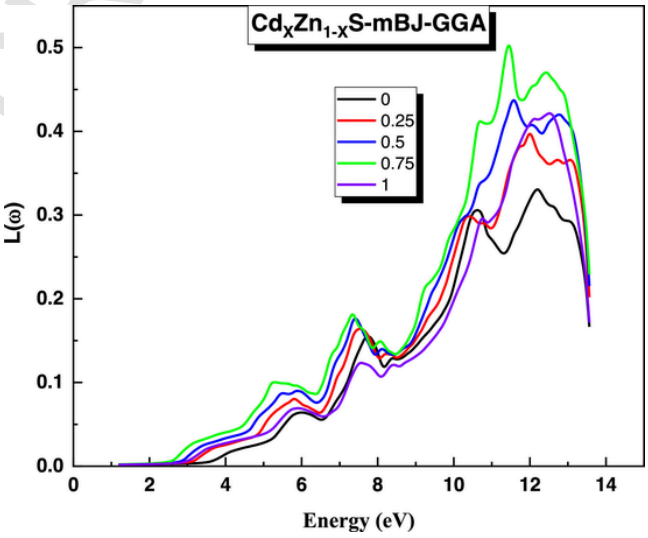

Fig. 6. Electron energy loss function L(ω) for $Cd_xZn_{1-x}S$ using mBJ-GGA method for $x = 0$, 0.25, 0.50, 0.75 and 1.

at different concentrations x between 0 and 1 were announced and discussed. The good accord between the present data and those communicated experimentally and theoretically is very satisfactory. For all $x = 0$, 0.25, 0.50, 0.75 and 1 existing materials, all their structures are zinc-blende with Γ structure. A predominant ionic type of the chemical bonding in these materials has been indicated. The DOS shows various peaks in both valence and conduction localities proposing that an abundance of conditions is obtainable for occupation. Within just about and in equidistant ultraviolet domains, the real frequency of the dielectric constant is bigger. However, the reverse can be seen in the far ultraviolet region. The common form of the real part of the dielectric constant is that looked forward to a harmonic oscillator. A principal peak of the real part of zinc-blende $Cd_xZn_{1-x}S$ appears at around 6 eV. The materials under load have been shown that they can be applied in optoelectronic domains.

Research data

No.

CRedit author contribution statement

S. Benlechheb: Did the computations.

M. Boucenna: Verified the analytical methods.

N. Bouarissa: Supervised the findings of this work and performed the computations.

Author contribution statement

All authors contributed equally to the paper.

Data availability statement

Data sharing not applicable to this article as no datasets were generated or analyzed during the current study.

Conflict of interest

There is no conflict of interest.

Data availability

No data was used for the research described in the article.

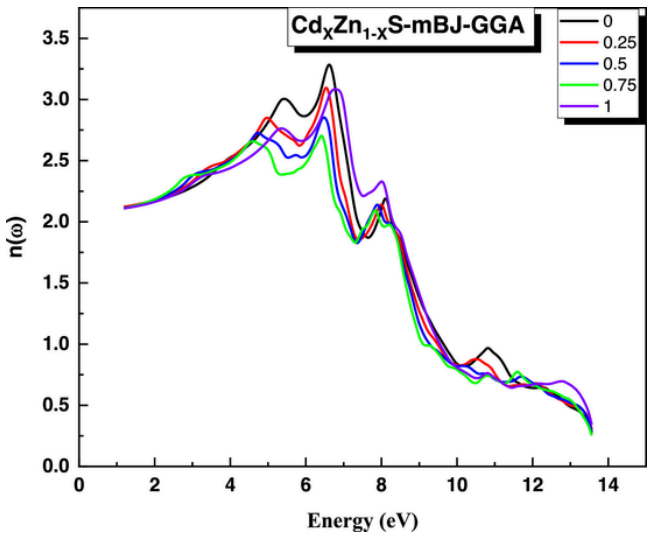

Fig. 7. Refractive index n(ω) for $Cd_xZn_{1-x}S$ using mBJ-GGA method for $x = 0$, 0.25, 0.50, 0.75 and 1.

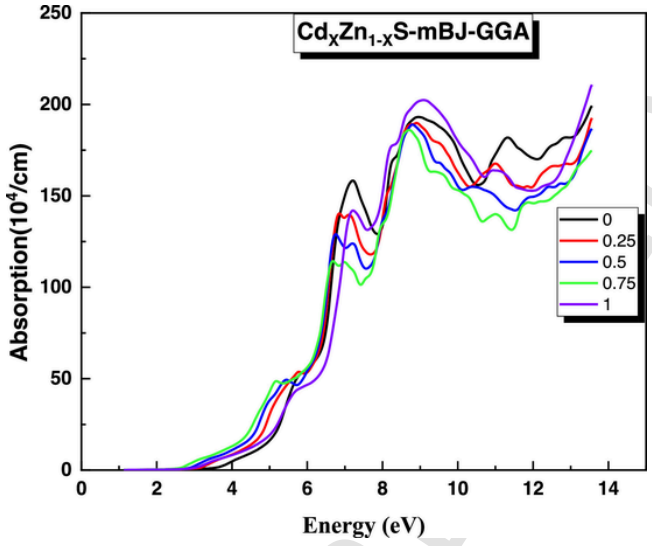

Fig. 8. Optical absorption coefficient α(ω) for $Cd_xZn_{1-x}S$ using mBJ-GGA method for $x = 0$, 0.25, 0.50, 0.75 and 1.

References

[1] M. Isshiki , J. Wang , Wide-bandgap II-VI semiconductors: growth and properties, in: S Kasap, P Capper (Eds.), Springer Handbook of Electronic and Photonic Materials, Springer Handbooks, Springer, Cham, 2017.
[2] V. Tomashyk, P. Feyehuk, L. Shcherbak, Ternary Alloys Based On II-VI Semiconductor Compounds, 1st edition, CRC Press, Boca Raton, 2013.
[3] X. Lei, C.H. Wong, E.A. Buntov, A.F. Zatsepin, G.J. Zhao, D.W. Boukhvalov, Optik (Stuttg) 178 (2019) 691.
[4] T. Hurma , Optik (Stuttg) 174 (2018) 324.
[5] R. Hernández Castillo, M. Acosta, I. Riech, G. Santana-Rodríguez, J. Mendes-Gamboa, C. Acosta, et al., Optik (Stuttg) 148 (2017) 95.
[6] F. Mezrag, W., N. Bouarissa, Physica B 405 (2010) 2272.
[7] N. Bouarissa, Physica B 399 (2007) 126.
[8] N. Bouarissa, Infrared Phys. Technol. 39 (1998) 265.
[9] A. Gueddim, S. Zerroug, N. Bouarissa, J. Lumin. 135 (2013) 243.
[10] D. W. Palmer Properties of the II-VI compound semiconductors 2019 .
[11] S. Q. Wang, Appl. Phys. Lett. 88 (2006) 061902.
[12] A. F. Wells, Structural Inorganic Chemistry, 5th edition, Oxford Science Publications, 1984, ISBN ISBN 0-19-855370-6.
[13] P. Klocek, Handbook of Infrared Optical Materials, CRC Press, 1991 ISBN 0-8247-8468-5.
[14] D. Lincot, G. Hodes, Chemical Solution Deposition of Semiconducting and Non-Metallic Films, in: Proceedings of the International Sympomisium, The Electrochemical Society, 2006 ISBN 1-56677-433-0.
[15] E. Wiberg, A.F. Holleman, Inorg Chem (2001) ISBN 0-12-352651-5.
[16] H. Zhao, A. Farah, D. Morel, C.S. Ferekides, Thin Solid Films 517 (2009) 2365.
[17] I.O. Oladeji, L. Chow, C.S. Ferekides, V. Viswanathan, Z. Zhao, Solar Energy Mater. Solar Cells 61 (2000) 203.
[18] T.D. Dzhafarov, F. Ongul, I. Karabay, J. Phys. D: Appl. Phys. 39 (2006) 3221.
[19] J.-.H Lee, W.-.C. Song, J.-.S. Yi, Y.-S.Yoo, Solar Energy Mater. Solar Cells 75 (2003) 227.
[20] M.C. Baykul, N. Orhan, Thin Solid Films 518 (2010) 1925.
[21] Y. Raviprakash, K.V. Bangera, G. K. Shivakumar, Solar Energy 83 (2009) 1645.
[22] K.U. Isah, N. Hariharan, A. Oberafo, Leonardo, J. Sci. 7 (2008) 111.
[23] V.B. Sanap, B. H. Pawar, J. Optoelectro. Biomedical Mater 3 (2011) 39.
[24] N.A. Al-Tememee, N.M. Saeed, S.M.A. Al-Dujayli, B. T.Chiad, Adv. Mater. Phys. Chem. 2 (2012) 19963.
[25] K. T. Ramakrishna Reddy, P. Jayarama Reddy, J. Phys. D: Appl. Phys. 25 (1992) 1345.
[26] K. W. Mitchell, A. L. Fahrenbruch, R. H. Bube, J. Appl. Phys. 48 (1977) 4365.
[27] B. M. Basol, J. Appl. Phys. 55 (1984) 601.
[28] J. Torres, G. Gordillo, Thin Solid Films 207 (1992) 231.
[29] T. Yamaguchi, J. Matsufusa, A. Yoshida, Jpn. J. Appl. Phys 31 (1992) L703.
[30] Y. Yamada, Y. Masumoto, J.T. Mullins, T. Taguchi, Appl. Phys. Lett. 61 (1992) 2190.
[31] K.B. Ozanyan, J.E. Nicholls, M. O'Neill, L. May, J.H.C. Hogg, W. E. Hagston, et al., Appl. Phys. Lett. 69 (1996) 4230.
[32] T. Tauchi, Y. Yamada, T. Ohno, J.T. Mullins, Y. Masumoto, Phys. Rev. B 191 (1993) 136.
[33] F. Zerarga, D. Allali, A. Bouhemadou, R. Khenata, B. Deghfel, S., R. Ahmed, Y. Al-Douri, S.S. Safaai, S. Bin-Omran, S. H. Naqib, Comput. Cond. Matter 32 (2022) e00705.
[34] A. Kleger, V. Meanier, Mater. Today Commun. 34 (2023) 105065.
[35] N.L. Lethole, P. Mukumbe, G. Makaka, J. Mag. Mag. Mater. 565 (2023) 170298.
[36] Y. Liu, X. Zhang, F. Wang, Chem. Phys. Lett. 806 (2022) 139992.
[37] S. Mehmood, Z. Ali, I. Ahmad, Mater. Chem. Phys. 295 (2023) 127164.
[38] S. Daoud, N. Bioud, N. Bouarissa, Mater. Sci. Semicond. Process 31 (2015) 124.
[39] N. Bouarissa, Mater. Sci. Semicond. Process 147 (2022) 106694.
[40] H. Heriche, Z. Rouabah, N. Bouarissa, Optik (Stuttg) 127 (2016) 11751.
[41] P. Chen, J.E. Nicholls, M. O'Neill, J.H.C. Hogg, B. Lunn, D.E. Ashenford, et al., Semicond. Sci. Technol 13 (1998) 1439.
[42] W. Schafer, M. Wegener, Semiconductor Optics and Transport Phenomena, Springer, Berlin, 2002.
[43] K. Kassali, N. Bouarissa, Microelectron. Eng 54 (2000) 277.
[44] N. Bouarissa, Mater. Chem. Phys. 124 (2010) 336.
[45] M.L. Cohen, J. R. Chelikowsky, Electronic Structure and Optical Properties of Semiconductors, Springer-Verlag, Berlin, 1989.
[46] J. Shi, H. Yan, X. Wang, Z. Feng, Z. Lei, C. Li, Solid-State Commun 146 (2008) 249.
[47] K. Nagamani, M.V. Reddy, Y. Lingappa, K T Ramakrishna Reddy, R W Miles, Int. J. Optoelectron. Eng 2 (2012) 1.
[48] A. Bouarissa, A. Gueddim, N. Bouarissa, S. Djellali, Polymer Bulletin 75 (2018) 3023.
[49] Z.Y. Feng, J.M. Zhang, J. Phys. Chem. Solids 114 (2018) 240.
[50] N. Bouarissa, S. Saib, J. Appl. Phys. 108 (2010), 113710 Erratum J. Appl. Phys. 111 (2012) 069901.
[51] S. Ferahtia, S. Saib, N. Bouarissa, S. Benyettou, Superlatt.Microstruct 67 (2014) 88.
[52] S. Chande, M. Debbarma, D. Ghosh, B. Debnath, S. Chattopadhyaya, Bull. Mater. Sci. 44 (2021) 97.
[53] M.A. Iqbal, A. Ahmad, M. Malik, J.R. Choi, P. K. Pham, Materials (Basel) 15 (2022) 2617.
[54] S. I. Sadovnikov, Int. J. Nanosci. 18 (2019) 1940060.
[55] N. Ul Aarifeen, A. Afaq, Mater. Chem. Phys. 251 (2020) 12309.
[56] N. Kaur, V. Srivastava, S.A. Dar, R. Khenata, R. Sharma, Mater. Sci. Eng. B 287 (2023) 116099.
[57] P. Hohenberg, W. Kohn, Phys. Rev. 136 (1964) B864.
[58] W. Kohn, L.J. Sham, Phys. Rev. 140 (1965) A1133.
[59] P. PBlaha, K. Schwars, G.K.H. Madsen, D. Kvasnicka, J. Luitz, in: Karlheinz Schwars (Ed.), WEIN2k, An Augmented Plane Wave + Local Orbitals Program for Calculating Crystal Properties, Techn, Universität, Wien, Austria, 2008, ISBN ISBN-3-9501031-1-2.
[60] H.J. Monkhorst, J.D. Pack, Phys. Rev. B 13 (1976) 5188.
[61] J.D. Pack, H.J. Monkhorst, Phys. Rev. B 16 (1977) 1748.
[62] L. Vegard, Z. Phys. 5 (1921) 17.
[63] M. Dadsetani, A. Pourghazi, Phys. Rev. B 73 (2006) 195102.
[64] H.R. Philipp, H. Ehrenreich, Phys. Rev 129 (1963) 1550.
[65] N. Bouarissa, Optik (Stuttg) 138 (2017) 263.
[66] Lattice constants, Argon National Laboratories (Advanced photon source), 2014
[67] X. Chen, X. Hua, J. Hu, J. Langlois, W.A. Goddard III, Phys. Rev. B 53 (1996) 1377.
[68] S. Wei, S.B. Zhang, Phys. Rev. B 62 (2000) 6944.
[69] F. Tran, P. Blaha, Phys. Rev. Lett. 102 (2009) 226401.
[70] U. Lunz, C. Schumacher, J. Nurnberger, K. Schull, A. Gerhard, U. Schüssler, et al., Semiconductor Sci. Technol. 12 (1997) 970.
[71] Y.P. Feng, K.L. Teo, M.F. Li, H.C. Poon, C.K. Ong, J.B. Xia, J. Appl. Phys. 74 (1993) 3948.
[72] Y.C. Cheng, X.I. Wu, J. Zhu, I.I. Xu, S.H. Li, P.K. Chu, J. Appl. Phys. 103 (2008) 073707.
[73] N. Bioud, K. Kassali, N. Bouarissa, J. Electron. Mater. 46 (2017) 2521.

[74] M.B. Askari, A.F. Kalourazi, M. Seifi, S.S. Shahangan, N. Askari, T.J. Manjili, Optik (Stuttg) 174 (2018) 154.
[75] N. Bouarissa, Physica B 406 (2011) 2583.
[76] H. Heriche, Z. Rouabah, N. Bouarissa, Int. J. Hydr. Energy 42 (2017) 9524.
[77] S. Adachi, Properties of Group-IV, III-V, and II-VI Semiconductors, Wiley, Chichester, 2005 and References Therein.
[78] S. Adachi, Properties of Semiconductor Alloys: Group-IV, III-V and II-VI Semiconductors, John Wiley & Sons Ltd., Chichester, and references therein, 2009.
[79] M. Boucenna, N. Bouarissa, F. Mezrag, Infrared Phys. Technol. 67 (2014) 318.
[80] X.Liu , J. K. Furbyna Optical dispersion of ternary II-VI semiconductor alloys, in Chalcogenide,2020
[81] M. Boucenna, N. Bouarissa, Optik (Stuttg) 125 (2014) 6611.
[82] P.Y. Yu, M. Cardona, Fundamentals of Semiconductors, Physics and Materials Properties, Springer-Verlag, Berlin, 1996.
[83] A. Bouarissa, A. Gueddim, N Bouarissa, H Maghraoui-Meherzi, Optik (Stuttg) 208 (2020) 164080.